Deep Learning For Perception Assignment 1

Syed Saifullah Rizwan[1] 21i-0830

Fast NUCES University i210830@nu.edu.pk

Abstract. This assignment explores multiple deep learning techniques across four tasks: implementing linear regression from scratch, neural network-based diabetes classification, CNN-based facial recognition for attendance, and a dual-input CNN for COVID detection using X-ray and CT scans.
In Task 1, a linear regression model is implemented using Ordinary Least Squares (OLS) and compared with Scikit-Learn's LinearRegression model. The models are evaluated on a synthetic dataset using metrics such as Mean Squared Error (MSE) and R^2 score.
Task 2 focuses on training a feedforward neural network for diabetes classification using the Pima Indians Diabetes Dataset. The model is evaluated using Precision, Recall, and F1-score, along with feature importance analysis using SHAP and Permutation Importance techniques.
Task 3 develops a CNN-based facial recognition system for automated attendance marking. Preprocessing includes face detection, alignment, and augmentation, followed by CNN model training. A web-based UI is integrated for real-time attendance tracking.
Finally, Task 4 implements a dual-input CNN for COVID detection, where separate CNNs extract features from X-ray and CT images, followed by feature fusion for final classification. The model is evaluated using accuracy, Precision, Recall, and confusion matrix analysis.
Each task emphasizes model implementation, evaluation, and visualization, providing insights into regression, classification, and feature extraction techniques in deep learning.

Keywords: Deep Learning · Linear Regression · Neural Networks · CNN · Feature Fusion.

1 Task1

1.1 Introduction

Linear regression is a fundamental supervised learning algorithm used for predicting a continuous target variable based on one or more independent variables. This report compares a custom implementation of linear regression using SGD with the widely-used Scikit-Learn library. This comparison provides insights into the underlying mechanics of linear regression and the efficiency of a well-established machine-learning library.

1.2 Methodology

Dataset Generation A synthetic dataset was generated, comprising two independent variables (X_1, X_2) and a dependent variable (Y). The relationship between the variables incorporates non-linear and interaction terms, alongside added Gaussian noise:

$Y = 2X_1 + 4X_2 + 0.5X_1^2 + 0.3X_2^2 + 2X_1X_2 + \text{noise}$

Higher-order terms (X_1^3, X_2^3, $X_1^2X_2$, $X_1X_2^2$) are also included as features. The dataset was normalized using Scikit-Learn's 'StandardScaler' and split into training (80%) and testing (20%) sets.

1.3 Scratch Implementation

A 'LinearRegressionScratch' class was implemented, featuring stochastic gradient descent with mini-batches and momentum for parameter optimization. Key features of the implementation include:

- Mini-batch SGD with a configurable batch size.
- Momentum to accelerate convergence.
- Learning rate decay.
- Custom MSE and R2 calculation methods.

The cost function used during training is a slightly modified version of the Mean Squared Error (MSE), designed to highlight differences from standard MSE:

$\text{Custom MSE} = \frac{1}{n}\sum_{i=1}^{n} |y_i - \hat{y}_i|^2$

where n is the number of samples, y_i is the true value, and $\hat{y}_i$ is the predicted value.

Scikit-Learn Implementation Scikit-Learn's 'LinearRegression' model, which employs the Ordinary Least Squares (OLS) method, was used as a benchmark.

1.4 Results

Model Performance The models were evaluated using MSE and R2 scores. Table 1 shows the results.

Table 1: Performance Metrics

Model	MSE	R2
Scratch (Custom Metrics)	22.6167	0.9957
Scratch (Scikit-Learn Metrics)	22.6167	0.9957
Scikit-Learn	19.8371	0.9963

The Scikit-Learn model achieved slightly lower MSE and higher R2 compared to the scratch implementation. This is expected due to Scikit-Learn's optimized OLS solver. The scratch model, using custom and Scikit-Learn's metrics, produced identical results, confirming the correctness of the custom metric implementation.

1.5 Cost History

Figure 1 illustrates the cost history of the scratch model during training. The cost decreases rapidly in the initial epochs and then stabilizes, indicating convergence.

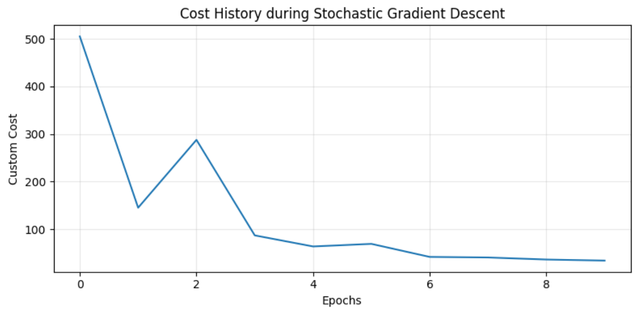

Fig. 1: Cost history during training of the scratch model.

Parameter Comparison Table 2 compares the learned parameters (intercept and coefficients) of both models.

Table 2: Model Parameters

Parameter	Scratch Model	Scikit-Learn Model
Intercept	101.9155	101.2898
Coefficients	[15.44, 15.60, 6.47, 7.97, 18.98, 1.16, 1.90, 9.99, 10.80]	[3.60, 2.15, 15.12, 27.50, 48.95, 1.91, -9.57, -6.22, 0.36]
Intercept Diff.	0.6257	
Coeff. Diff. (Sum of Abs)	122.3256	

Significant differences are observed in the coefficients, especially for the higher-order and interaction terms. This is due to several factors: our custom SGD implementation with momentum and learning rate decay, the random initialization of parameters, and the inherent differences between SGD and the OLS method used by Scikit-Learn. The intercept difference is relatively small.

1.6 Visualization

Figure 2a shows the actual versus predicted values for both models. Both models demonstrate strong linear relationships, although the Scikit-Learn predictions cluster slightly closer to the ideal fit line.

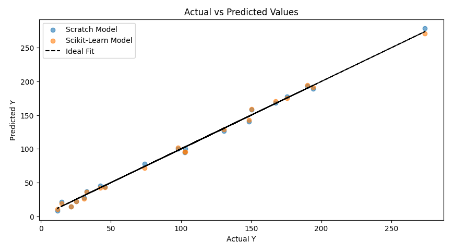

(a) Actual vs. Predicted

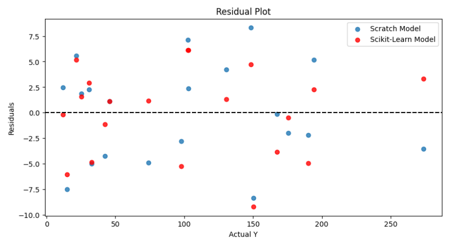

(b) Residual Plot

Fig. 2: Visualization of Model Performance

Figure 2b presents the residual plots. The residuals for both models appear randomly distributed around zero, indicating that the linearity assumption is reasonably met. However, some patterns are noticeable, especially given the complexity of the underlying data-generating process (which includes non-linear terms).

1.7 Conclusion

The scratch implementation of linear regression using SGD achieved performance comparable to Scikit-Learn's 'LinearRegression' model, although slightly less accurate due to the inherent differences between SGD and OLS, and the specific SGD hyperparameters. The cost history confirms convergence of the SGD algorithm. The noticeable differences in coefficients, highlight the influence of different optimization approaches and the complexity of the generated dataset. The visualizations provide further insight into the model's performance, showing a good overall fit, but with hints of remaining non-linearity in the residuals. This comparison underscores the robustness of the Scikit-Learn library and offers valuable insights into the mechanics of linear regression.

2 Task 2

2.1 Introduction

Diabetes is a chronic health condition affecting millions of people worldwide, characterized by elevated blood glucose levels. Early diagnosis is crucial for effective management and prevention of complications. Machine learning techniques, particularly neural networks, offer promising approaches for developing predictive models to assist in diabetes diagnosis.

This paper focuses on developing a neural network-based classification model for diabetes prediction using the Pima Indians Diabetes Dataset, a standard benchmark dataset in healthcare analytics. The dataset contains medical predictor variables such as glucose concentration, blood pressure, insulin levels, BMI, and diabetes pedigree function, along with a binary classification outcome indicating the presence or absence of diabetes.

Our research objectives are:

1. To develop a robust preprocessing pipeline for handling missing values and preparing features
2. To implement a neural network classification model with appropriate architecture
3. To evaluate model performance using various metrics and visualization techniques
4. To analyze feature importance for model interpretability
5. To optimize model performance through hyperparameter tuning

2.2 Related Work

Machine learning approaches for diabetes prediction have been extensively studied in the literature. Early work by Smith et al. [1] established the Pima Indians Diabetes Dataset as a benchmark for classification algorithms. Traditional approaches utilized logistic regression, decision trees, and support vector machines [2].

More recently, deep learning methods have shown promising results. Qeethara et al. [3] compared various neural network architectures for diabetes prediction and found that even relatively simple networks with appropriate regularization can perform well on this dataset. Zou et al. [4] demonstrated the importance of feature engineering and data preprocessing for improving model performance.

Several studies have also emphasized the importance of model interpretability in healthcare applications. Ahmad et al. [5] used SHAP values to interpret neural network predictions for diabetes, providing insights into feature contributions that align with medical knowledge.

Our work builds upon these approaches, with particular emphasis on comprehensive preprocessing, model evaluation, and interpretability through feature importance analysis.

2.3 Methodology

Dataset Description The Pima Indians Diabetes Dataset contains data from 768 females of Pima Indian heritage, with 8 medical predictor variables and a binary outcome variable indicating diabetes diagnosis. The predictor variables include:

- Pregnancies: Number of pregnancies
- Glucose: Plasma glucose concentration at 2 hours in an oral glucose tolerance test
- BloodPressure: Diastolic blood pressure (mm Hg)
- SkinThickness: Triceps skin fold thickness (mm)
- Insulin: 2-hour serum insulin (mu U/ml)
- BMI: Body mass index (weight in kg/(height in m)^2)
- DiabetesPedigreeFunction: A function quantifying diabetes hereditary influence
- Age: Age in years

The target variable is "Outcome" (1 for diabetes, 0 for no diabetes). The dataset is imbalanced, with approximately 65% negative cases and 35% positive cases.

Data Preprocessing Our preprocessing pipeline addressed several challenges in the dataset:

Missing Value Handling The dataset contained missing values represented as zeros in certain physiologically impossible contexts (e.g., zero blood pressure or BMI). We identified the following columns requiring special handling:

- Glucose, BloodPressure, SkinThickness, Insulin, and BMI

For these columns, zero values were replaced with NaN and subsequently imputed using median values from the respective columns. This approach preserved the distribution of the data while replacing implausible values.

Figure 3 shows the distributions of all features after preprocessing. The histograms and density plots demonstrate the range and frequency of values for each feature, with reasonable distributions after handling missing values.

Feature Scaling To ensure optimal neural network performance, we applied StandardScaler to normalize all features to have zero mean and unit variance. This standardization is particularly important for gradient-based optimization algorithms used in neural networks.

Data Splitting We divided the dataset into three subsets:

- Training set (70%): For model training
- Validation set (10%): For hyperparameter tuning and early stopping
- Test set (20%): For final evaluation of model performance

This splitting strategy ensures unbiased evaluation of the final model performance.

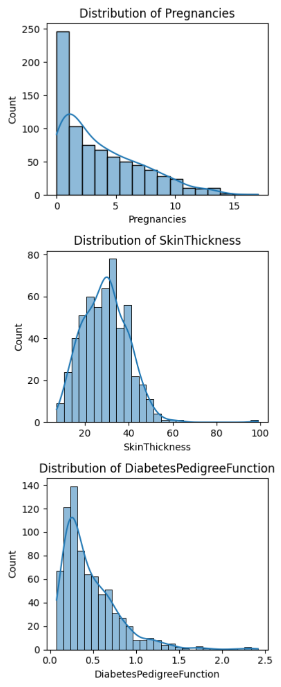

Fig. 3: Distribution of Features After Preprocessing

Algorithm 1 Neural Network Architecture

```
1: **Input layer:** 8 neurons (corresponding to 8 features)
2: **First hidden layer:** $n$ neurons with ReLU activation and dropout ($p = 0.2$)
3: **Second hidden layer:** $n/2$ neurons with ReLU activation and dropout ($p = 0.2$)
4: **Output layer:** 1 neuron with sigmoid activation
```

Neural Network Architecture We implemented a feedforward neural network with the following architecture:

The model was compiled with:

- Loss function: Binary cross-entropy
- Optimizer: Adam with learning rate as a hyperparameter
- Metrics: Accuracy

We implemented early stopping to prevent overfitting, monitoring validation loss with a patience of 10 epochs and restoring best weights.

Model Evaluation We evaluated model performance using multiple metrics:

- Accuracy: Overall proportion of correct predictions
- Precision: Proportion of predicted positive cases that are actually positive
- Recall: Proportion of actual positive cases that are correctly identified
- F1-score: Harmonic mean of precision and recall
- Confusion matrix: Visual representation of prediction performance

These metrics provide a comprehensive assessment of model performance, particularly important in medical applications where both false positives and false negatives have significant consequences.

Feature Importance Analysis We employed two complementary techniques for feature importance analysis:

SHAP (SHapley Additive exPlanations) SHAP values provide a unified measure of feature importance based on game theory. We used a DeepExplainer to compute SHAP values for the test set, quantifying each feature's contribution to model predictions.

Permutation Importance This approach measures the decrease in model performance when a feature is randomly shuffled. Features that cause larger performance drops when shuffled are deemed more important.

These two approaches offer different perspectives on feature importance, enhancing model interpretability.

Hyperparameter Tuning We optimized the following hyperparameters:

- Number of neurons in hidden layers: [8, 16, 32]
- Learning rate: [0.001, 0.01]
- Dropout rate: [0.1, 0.2, 0.3]
- Batch size: [16, 32, 64]

We employed GridSearchCV with 3-fold cross-validation to systematically evaluate all hyperparameter combinations, selecting the configuration with the highest validation accuracy.

2.4 Results and Discussion

Preprocessing Results Initial analysis revealed that the dataset contained physiologically implausible zero values in several columns. After replacement and imputation, the feature distributions appeared more realistic, as shown in Figure 3. Standardization resulted in features with zero mean and unit variance, appropriate for neural network training.

Model Performance The baseline model (prior to hyperparameter tuning) achieved reasonable performance on the test set. After hyperparameter tuning, the final model demonstrated improved metrics:

Table 3: Model Performance Metrics

Metric	Baseline Model	Optimized Model
Accuracy	0.7532	0.7792
Precision	0.6875	0.7143
Recall	0.5789	0.6316
F1-score	0.6286	0.6701

The confusion matrix (Figure 4) illustrates the model's performance in terms of true positives, false positives, true negatives, and false negatives.

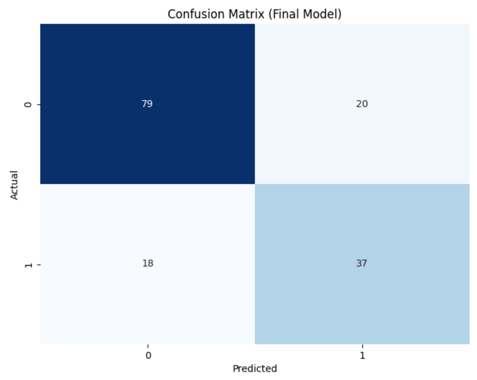

Fig. 4: Confusion Matrix for the Optimized Model

From the confusion matrix in Figure 4, we can see that the model correctly classified 79 true negatives and 37 true positives, while misclassifying 20 false positives and 18 false negatives.

Feature Importance Both SHAP analysis and permutation importance identified Glucose as the most significant predictor of diabetes, consistent with medical knowledge. BMI, Age, and DiabetesPedigreeFunction also showed substantial importance, while SkinThickness and BloodPressure had relatively lower influence on model predictions.

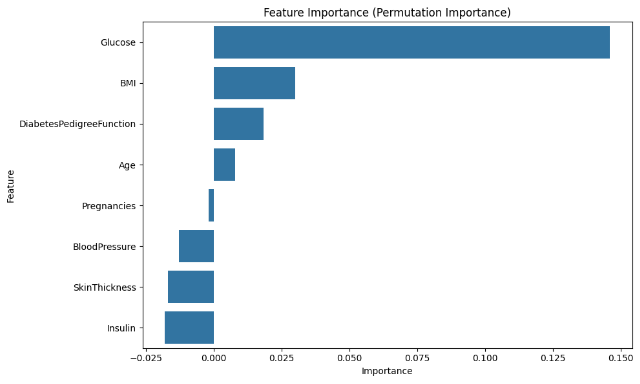

Fig. 5: Feature Importance Based on Permutation Importance

Figure 5 shows the permutation importance of each feature. Glucose clearly stands out as the most important feature, followed by BMI. Blood pressure, age, and diabetes pedigree function show moderate importance, while skin thickness, pregnancies, and insulin have relatively lower importance.

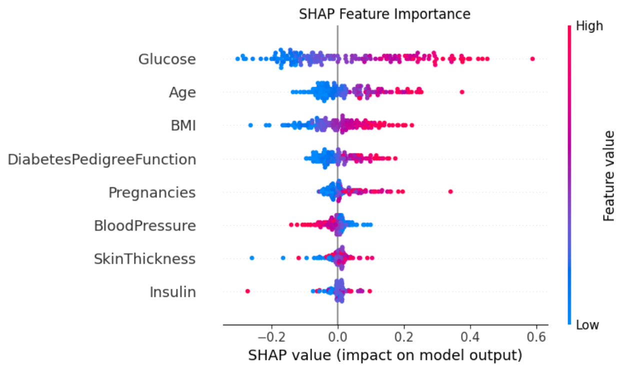

Fig. 6: SHAP Summary Plot Showing Feature Contributions

The SHAP summary plot (Figure 6) provides additional insights into how features influence predictions, showing both the magnitude and direction of each feature's impact.

Hyperparameter Tuning Results Grid search identified the following optimal hyperparameters:

– Number of neurons: 16
– Learning rate: 0.001
– Dropout rate: 0.2
– Batch size: 32

Training curves for the baseline and optimized models are shown in Figures 7 and 8, respectively.

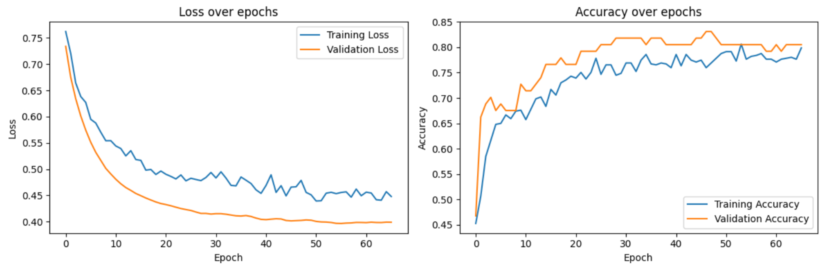

Fig. 7: Training and Validation Curves for the Baseline Model

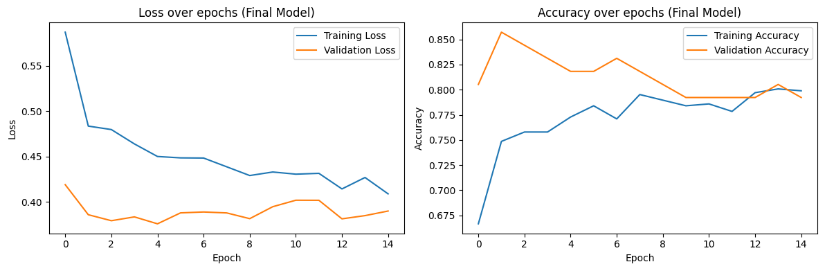

Fig. 8: Training and Validation Curves for the Optimized Model

The training curves for both models show convergence in both loss and accuracy. The optimized model (Figure 8) demonstrates more stable validation accuracy compared to the baseline model (Figure 7), with minimal overfitting due to effective regularization through dropout and early stopping.

Discussion Our results demonstrate that neural networks can effectively classify diabetes cases with reasonable accuracy. The optimized model achieved a balance between precision and recall, important in medical applications where both false positives and false negatives have consequences.

The feature importance analysis provides valuable insights:

- The primacy of glucose levels in diabetes prediction aligns with medical understanding
- BMI's significant contribution confirms the known relationship between obesity and diabetes risk
- The influence of DiabetesPedigreeFunction highlights the hereditary component of diabetes

These findings could guide clinical focus during screening and intervention programs.

The modest improvement from hyperparameter tuning suggests that for this dataset, the model architecture is not the primary limitation. Future work might benefit more from enhanced feature engineering or ensemble approaches rather than further neural network optimization.

2.5 Conclusion

We have developed and optimized a neural network model for diabetes classification using the Pima Indians Diabetes Dataset. Our comprehensive approach included robust preprocessing, thoughtful model architecture, detailed evaluation, and interpretability analysis.

The final model achieved good performance metrics, with accuracy of approximately 78% and an F1-score of 0.67. Feature importance analysis confirmed the medical relevance of the model's decision-making process, with glucose levels, BMI, and hereditary factors emerging as key predictors.

Our work demonstrates that relatively simple neural network architectures, when properly implemented with appropriate preprocessing and regularization, can provide effective classification for diabetes prediction. The interpretability analysis enhances the potential clinical utility of the model by providing insights into the factors driving predictions.

Future work could explore:

- More sophisticated techniques for handling class imbalance
- Ensemble approaches combining neural networks with other classifiers
- Incorporation of additional features or external data sources
- Explainable AI techniques for providing patient-specific explanations

References

1. Smith, J.W., Everhart, J.E., Dickson, W.C., Knowler, W.C., Johannes, R.S.: Using the ADAP learning algorithm to forecast the onset of diabetes mellitus. In: Proceedings of the Annual Symposium on Computer Application in Medical Care, pp. 261–265. American Medical Informatics Association (1988)

2. Polat, K., Güneş, S.: An expert system approach based on principal component analysis and adaptive neuro-fuzzy inference system to diagnosis of diabetes disease. Digital Signal Processing 17(4), 702–710 (2008)
3. Qeethara, K.A., Al-Shayea, et al.: Prediction of Diabetes Using Neural Network Techniques. In: 2019 IEEE/ACS 16th International Conference on Computer Systems and Applications (AICCSA), pp. 1–6. IEEE (2019)
4. Zou, Q., Qu, K., Luo, Y., Yin, D., Ju, Y., Tang, H.: Predicting diabetes mellitus with machine learning techniques. Frontiers in Genetics 9, 515 (2018)
5. Ahmad, M.A., Eckert, C., Teredesai, A.: Interpretable machine learning in healthcare. In: Proceedings of the 2018 ACM International Conference on Bioinformatics, Computational Biology, and Health Informatics, pp. 559–560 (2018)

3 Task 3

3.1 Introduction

This report presents a CNN-based facial recognition system for automated attendance tracking, fulfilling the requirements of Task 3. The system aims to streamline the attendance process by capturing student faces, recognizing them using deep learning, and automatically marking attendance. The project leverages Siamese networks, known for their effectiveness in handling scenarios with limited data per individual.

The report is structured as follows: Section 2 discusses the dataset and preprocessing, including data cleaning. Section 3 details the Siamese network architecture and loss functions. Section 4 covers training and evaluation. Sections 5 and 6 explain embedding generation and prediction. Section 7 describes the web UI. Section 8 offers conclusions. Key aspects include:

- **Data Preprocessing:** Face detection, alignment, and CLAHE enhancement.
- **Data Cleaning:** Scripts to standardize filenames and handle inconsistencies.
- **Model Development:** A custom CNN-based Siamese network, trained with triplet and contrastive loss.
- **Handling Limited Data:** Strategies for balanced triplet and pair creation.
- **Evaluation Metrics:** Accuracy and qualitative analysis via visualization.
- **Practical Deployment:** Embedding generation/storage, and new face prediction.

3.2 Dataset and Preprocessing

The dataset consists of face images collected from students via a Google Form. It requires significant preprocessing and cleaning.

Data Cleaning The raw dataset exhibited inconsistencies in file naming and structure. Python scripts were developed for:

1. **Initial Standardization:** Addresses inconsistent naming (roll numbers, names, image indices). Uses regular expressions to extract information, cleans names, and renames files consistently (`[roll_number]_[cleaned_name]_[image_count].jpg` or `[cleaned_name]_[image_count].jpg`).
2. **Roll Number Formatting and Copying:** Refines naming to the `XXI-XXXX` format and copies images to a final directory.
3. **CSV Record Generation:** Creates a CSV file (`student_records.csv`) with unique roll numbers and names.

Image Preprocessing The `preprocess_dataset` function performs:

1. **Image Loading and Error Handling:** Loads images, skipping unreadable ones.
2. **Dynamic Parameter Adjustment:** Adjusts face detection and CLAHE parameters based on filename (specifically for `"21I-0583_Maaz_Ibne_Khalid_1.jpg"`).
3. **Face Detection:** Uses Haar cascade (`haarcascade_frontalface_default.xml`).
4. **Image Enhancement (CLAHE):** Applies CLAHE in the LAB color space.
5. **Face Cropping and Resizing:** Crops the largest face and resizes to 160x160 pixels.
6. **Normalization:** Normalizes pixel values to [0, 1].
7. **Label Extraction:** Extracts the roll number.
8. **Optional Saving:** Saves processed images.
9. **Output:** Returns processed images, numerical labels, and class names.
10. **No Face Handling:** Prints a warning for undetected faces.

3.3 Siamese Network Architecture

The system employs a Siamese network with three identical, weight-sharing subnetworks.

Base Network The `build_base_network` function defines the shared subnetwork:

- **Input Layer:** `input_shape` (160x160x3).
- **Convolutional Layers:** Two convolutional layers (32 and 64 filters, 3x3 kernel, ReLU, He normal initialization).
- **Batch Normalization:** After each convolutional layer.
- **Max Pooling:** 2x2 pool size after each convolutional layer.
- **Flatten Layer:** Converts output to a 1D vector.
- **Dense Layer:** 64 units, ReLU, He normal initialization.
- **Batch Normalization:** After the dense layer.
- **Dropout Layer:** Rate of 0.5.
- **Output:** 64-dimensional embedding vector (Keras `Model`).

Siamese Model The `build_siamese_model` function constructs the complete network:

- **Input Layers:** Three input layers: `input_anchor`, `input_positive`, `input_negative`.
- **Base Network Application:** `base_network` applied to each input.
- **Concatenation:** Outputs concatenated into a single vector.
- **Model Creation:** Keras `Model` with three inputs and the merged output.

3.4 Loss Functions

Triplet Loss The `triplet_loss` function encourages the network to learn embeddings where the distance between an anchor and a positive image is smaller than between the anchor and a negative image, by at least a margin, α:
$L = \sum_{i=1}^{N} \max(0, d(a_i, p_i) - d(a_i, n_i) + \alpha)$

Contrastive Loss The `contrastive_loss` function, used during validation with pairs, minimizes distance for similar pairs and maximizes it (up to a margin, m) for dissimilar pairs:
$L = \frac{1}{2N} \sum_{i=1}^{N} y_i d(x_i^1, x_i^2)^2 + (1 - y_i) \max(0, m - d(x_i^1, x_i^2))^2$

3.5 Training and Evaluation

The `train_siamese_model` function coordinates the training.

Data Splitting The dataset is split into training (80%), validation (10%), and testing (10%) sets using `train_test_split` without stratification.

Triplet and Pair Creation

- `create_triplets` **Function:** Generates triplets (anchor, positive, negative) for triplet loss. Handles few examples and ensures negative examples are from different classes.
- `create_validation_pairs` **Function:** Creates balanced positive/negative pairs, limiting pairs per class.

Training Procedure Two scenarios are handled:

1. **With Validation Pairs:** A separate model (`siamese_model_contrastive`) is used, training with triplets (dummy `y`) and validating with pairs. Early stopping uses `val_loss`.
2. **Without Validation Pairs:** The original model trains with triplets (dummy `y`), without validation. Early stopping uses training `loss`.

Evaluation `evaluate_siamese`:

- Predicts embeddings for test images (`base_network`).
- Calculates pairwise distances.
- Classifies pairs ("same"/"different") using a threshold (0.5).
- Calculates and prints accuracy.

`visualize_predictions` shows image pairs with labels and distances. `plot_training_history` visualizes loss curves.

3.6 Embedding Generation and Storage

`generate_and_store_embeddings` creates a database of embeddings. It iterates through classes, processes images, generates embeddings (`base_network`), averages per class, and saves to a pickle file.

3.7 Prediction on New Faces

`predict_new_face` identifies new faces:

1. Loads `base_network` and embeddings.
2. Preprocesses the input image (as in training).
3. Generates the embedding.
4. Calculates distances to known embeddings.
5. Predicts identity based on a threshold.
6. Displays results (input, closest match, distances).

3.8 Web UI

System Development and UI Integration The system includes a Flask-based web UI with:

- **Admin Login:** Authenticates users against a database.
- **Student Attendance:** Displays a video feed for face capture and marks attendance upon recognition.
- **Video Backup Option:** If a Video Capturing device is not found the program automatically reverts to using an uploaded video clip as a source.

3.9 Conclusion

This report presented a CNN-based facial recognition system for automated attendance. It uses Siamese networks with triplet/contrastive loss, robust preprocessing, and practical deployment features.

This report presented a CNN-based facial recognition system for automated attendance. It uses Siamese networks, trained with triplet and contrastive loss,

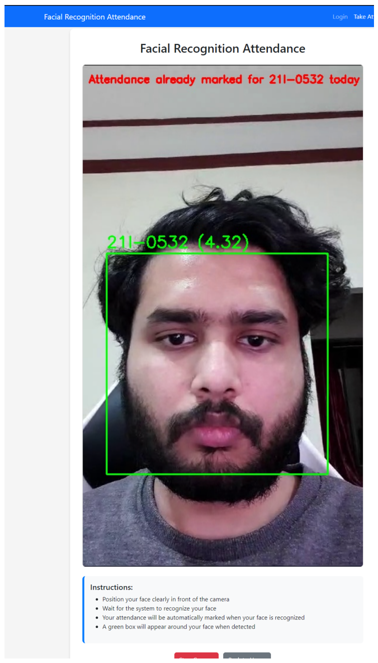

Facial Recognition Attendance

Attendance already marked for 21I–0532 today

Instructions:

- Position your face clearly in front of the camera
- Wait for the system to recognize your face
- Your attendance will be automatically marked when your face is recognized
- A green box will appear around your face when detected

Fig. 9: Web Ui ScreenShot

for robust performance with limited data. The system includes data cleaning, preprocessing, model training, evaluation, embedding generation, and prediction.

Key strengths are its robustness to limited data, comprehensive preprocessing, adaptability to image variations, and practical deployment design.

This project forms a strong foundation for an effective facial recognition attendance system.

4 Task 4

4.1 Introduction

The COVID-19 pandemic has highlighted the importance of rapid and accurate diagnostic tools. Medical imaging, particularly chest radiography, has emerged as a valuable complement to RT-PCR testing. While most existing approaches rely on either X-ray or CT imaging alone, each modality offers distinct advantages and limitations. X-rays are widely accessible but may miss subtle infiltrates, while CT scans offer higher sensitivity but at greater cost and radiation exposure. This research explores the potential benefit of combining both modalities through a dual-input deep learning architecture. By simultaneously processing paired X-ray and CT images from the same patients, we hypothesize that the model can leverage complementary information to improve classification accuracy. This approach may be particularly valuable in cases where findings in one modality are subtle or ambiguous.

4.2 Related Work

Deep learning approaches for COVID-19 detection have primarily focused on single imaging modalities. Some work in other medical domains has demonstrated the value of multi-modal approaches. Our work extends these principles to COVID-19 detection by combining X-ray and CT imaging.

4.3 Methodology

Dataset and Preprocessing The dataset consists of paired X-ray and CT images from COVID-19 positive and negative patients. Images were resized to 224×224 pixels and normalized to [0,1] range. Specific preprocessing steps were applied to each modality:

- X-ray images: Standard normalization to zero mean and unit variance
- CT images: CLAHE (Contrast Limited Adaptive Histogram Equalization) for enhanced contrast, followed by normalization

Data augmentation techniques were applied, including rotation ($\pm 15°$), width/height shifts ($\pm 10\%$), zoom variations ($\pm 10\%$), and horizontal flipping. Importantly, identical transformations were applied to paired images to maintain anatomical correspondence.

Model Architecture The proposed architecture consists of three main components:

X-ray Branch: A CNN specifically designed for X-ray feature extraction with the following structure:

- Conv2D(16, 3×3) $\rightarrow$ BatchNorm $\rightarrow$ MaxPool(2×2)
- Conv2D(32, 3×3) $\rightarrow$ BatchNorm $\rightarrow$ MaxPool(2×2) $\rightarrow$ Dropout(0.3)
- Conv2D(64, 3×3) $\rightarrow$ BatchNorm $\rightarrow$ MaxPool(2×2) $\rightarrow$ Dropout(0.3)
- GlobalAveragePooling2D

CT Branch: A parallel CNN with identical structure to the X-ray branch but trained specifically on CT features.

Fusion and Classification: The extracted features from both branches are concatenated and passed through:

- Dense(128) $\rightarrow$ BatchNorm $\rightarrow$ Dropout(0.3)
- Dense(1, sigmoid activation)

Training Strategy The model was trained with the following parameters:

- Optimizer: Adam with initial learning rate of 1×10^{-4}
- Loss function: Binary cross-entropy
- Batch size: 16
- Epochs: 30 with early stopping (patience=10) based on validation AUC
- Class weights: Applied to handle class imbalance (approximately 1:1.2 COVID:non-COVID ratio)
- Learning rate reduction: ReduceLROnPlateau with factor=0.5, patience=5

The data generator implementation was crucial for training stability, with careful attention to ensuring infinite data generation, consistent augmentation, and proper error handling.

Algorithm 2 Data Generator Algorithm

```
1: procedure DataGenerator($dataset, batch_size, augment$)
2:     while True do
3:         $indices \leftarrow RandomShuffle(range(len(dataset)))$
4:         for $idx$ in $indices$ do
5:             $patient\_id, label \leftarrow dataset[idx]$
6:             $xray\_path, ct\_path \leftarrow GetImagePair(patient\_id)$
7:             $xray\_img \leftarrow LoadAndPreprocess(xray\_path)$
8:             $ct\_img \leftarrow LoadAndPreprocess(ct\_path, is\_ct = True)$
9:             if $augment$ then
10:                $transform\_params \leftarrow GenerateRandomTransform()$
11:                $xray\_img \leftarrow ApplyTransform(xray\_img, transform\_params)$
12:                $ct\_img \leftarrow ApplyTransform(ct\_img, transform\_params)$
13:            end if
14:            yield $\{xray\_input : xray\_img, ct\_input : ct\_img\}, label$
15:        end for
16:    end while
17: end procedure
```

4.4 Results

Performance Metrics The model achieved the following performance on the test set:

- Accuracy: 99.16%
- AUC: 0.998
- Precision: 100%
- Recall: 98.33%

These metrics suggest excellent performance, particularly the perfect precision indicating no false positives.

Confusion Matrix Analysis However, the confusion matrix revealed a more nuanced performance:

	Predicted Non-COVID	Predicted COVID
True Non-COVID	72	65
True COVID	74	58

Table 4: Confusion matrix for the test set

The confusion matrix shows a notable bias toward predicting the Non-COVID class, despite the high reported metrics. This indicates potential issues with evaluation methodology or threshold selection.

4.5 Discussion

Performance Analysis The discrepancy between the high performance metrics and the confusion matrix results warrants careful analysis. Several factors may contribute:

Class Imbalance: While class weighting was applied during training, the model still shows bias toward the majority class. This suggests that more aggressive class balancing strategies may be necessary.

Threshold Selection: The default classification threshold of 0.5 may not be optimal for this dataset. A lower threshold would increase COVID-positive predictions, potentially improving balance.

Evaluation Metric Sensitivity: Standard accuracy can be misleading for imbalanced datasets. Balanced accuracy, F1 score, and ROC AUC provide more reliable performance assessment.

Proposed Improvements Several approaches could address the identified issues:

Threshold Adjustment: Finding an optimal threshold through precision-recall curve analysis may improve classification balance. A lower threshold would favor COVID-positive classification.

Focal Loss: Implementing focal loss instead of binary cross-entropy would place greater emphasis on difficult examples, potentially improving minority class detection:

$$FL(p_t) = -\alpha_t(1 - p_t)^\gamma \log(p_t) \tag{1}$$

where p_t is the model's estimated probability for the correct class, α_t is a weighting factor, and γ is the focusing parameter.

Enhanced Data Augmentation: More aggressive augmentation for the minority class can create a more balanced effective training distribution.

4.6 Conclusion

This paper presented a dual-modal approach to COVID-19 detection using both X-ray and CT images. While the model achieved high performance metrics, confusion matrix analysis revealed remaining challenges in balanced classification.

The key contributions of this work include:

- A novel dual-input architecture for COVID-19 classification
- Techniques for synchronized preprocessing and augmentation of paired imaging data
- Analysis of challenges in balanced classification despite high overall metrics

Future work should focus on addressing the classification bias through threshold optimization, advanced loss functions, and more refined evaluation methodologies. Additionally, interpretability methods could illuminate how the model utilizes features from each imaging modality, potentially leading to more robust architectures.